ELSEVIER

Physica C 372–376 (2002) 7–10

PHYSICA C

www.elsevier.com/locate/physc

Properties of SNS Josephson junctions with HfTi interlayers

D. Hagedorn *, R. Dolata, F.-Im. Buchholz, J. Niemeyer

Physikalisch-Technische Bundesanstalt, Bundesallee 100, 38116 Braunschweig, Germany

Abstract

The fabrication process in superconductor–normal metal–superconductor (SNS) technology has been improved to raise the characteristic voltage of SNS active elements. Josephson junctions with normal metal interlayers made from HfTi were realized in ramp-type design with dimensions down to the deep sub-micron range. To investigate the influence of the interfaces, junctions with different sequences of interim layers were fabricated, according to Nb/HfTi/Nb trilayer and Nb/HfTi–Nb–HfTi/Nb multilayer structures. Typical values of the characteristic voltage and the critical current density are $V_c = 107$ μV and $j_c = 550$ kA/cm^2 for Nb/HfTi/Nb junctions and $V_c = 460$ μV and $j_c = 210$ kA/cm^2 for Nb/HfTi–Nb–HfTi/Nb junctions, each for areas of $A = 0.2$ μm^2. The junctions were experimentally investigated for the temperature dependence of critical currents, the influence of externally applied magnetic fields, and the application of microwave power.

Keywords: Josephson effect; SNS technology; Superconducting electronics

1. Introduction

The technological process used at PTB for ramp-designed SNS junctions offers the possibility of producing miniaturized Josephson junctions in sub-micron sizes [1,2]. For Nb-based junctions, the use of HfTi as N-material has proved advantageous resulting from improved adhesive properties. Nb/HfTi/Nb ramp junctions have proved reliable in large series arrays containing 10,000 junctions (single contact area $A < 0.4$ μm^2, N-layer thickness $d = 40$ nm, $V_c = 2.4$ μV, $j_c = 10$ kA/cm^2). Under 1.5 GHz radiation, it was demonstrated that each single junction contributed to the expected constant voltage steps [3]. With a reduced thickness ($d = 20$ nm) of the HfTi layer an increase of both, V_c(107 μV) and j_c (550 kA/cm^2), was achieved. For digital circuit application, this would result in $I_c \approx 100$ μA and $R_N \approx 1$ Ω when scaled down to $A = 0.02$ μm^2.

2. Fabrication of SNS ramp-type junctions

The fabrication process is based on a combination of standard non-contact lithography and etching techniques. First, on a three inch silicon substrate, an Al_2O_3 etch stop layer, the Nb base layer, and an SiO_2 insulation layer are sputtered. Photoresist is spun onto the wafer and exposed using an optical wafer stepper. Contact free lithography guarantees sharp edges, which are necessary for the production of ramp junctions. In a first

* Corresponding author. Fax: +49-531-592-2130.
E-mail address: daniel.hagedorn@ptb.de (D. Hagedorn).

0921-4534/02/$ - see front matter © 2002 Elsevier Science B.V. All rights reserved.
PII: S0921-4534(02)00688-3

CF_4/O_2 reactive ion etching process, the ramps are formed as the resist withdraws under the influence of oxygen [4,5]. Then, the remaining resist is removed. Right before the N-layer and the Nb wiring are sputtered, the ramps are cleaned for 2 min in an Ar plasma (cleaning times of 4 or 6 min showed no changes in the junctions' properties). The wiring is patterned using PMMA resist and e-beam lithography. A 30 nm Cr layer is lifted off the PMMA to form a hard etch mask. Then, the Nb wiring is reactive ion etched, followed by an Ar beam etching of the N-layer. Compared with a process to fabricate conventional planar junctions, the ramp process is faster because only two lithographic steps are required for fabricating the junctions [3].

3. Measurement and results

To investigate the influence of the interfaces between different materials within the SNS junction assembly, various types of junctions with different sequences of interim layers were realized (a) with a common SNS structure, i.e. Nb/HfTi/Nb, and (b) with multilayer SN′S structures, i.e. Nb/HfTi–Al–HfTi/Nb and Nb/HfTi–Nb–HfTi/Nb. All measurements were carried out at $T = 4.2$ K. All given data are based on at least two different wafers and multiple chips. Introduction of an (HfTi–Al–HfTi) N′-multilayer sequence between the Nb electrodes leads to a slight increase in V_c compared to junctions with a uniform HfTi N-layer, which is mainly due to a higher critical current. In contrast, when an N′ (HfTi–Nb–HfTi) multilayer sequence is introduced, considerable differences from common SNS-type HfTi junctions are apparent: Nb/HfTi–Nb–HfTi/Nb multibarrier junctions with thicknesses of the inner N′-multilayer of HfTi(5 nm)–Nb(10 nm)–HfTi(5 nm) exhibit a 4.5 times higher characteristic voltage, $V_c = 460$ µV and a 2.5 times smaller critical current density, $j_c = 210$ kA/cm^2 (compared with Nb/HfTi/Nb junctions with an N-layer thickness of $d = 20$ nm). This would result in $I_c \approx 100$ µA and $R_N \approx 4.6$ Ω when scaled down to $A = 0.05$ µm^2. However, linearity in scaling has been achieved only down to $A = 0.2$ µm^2.

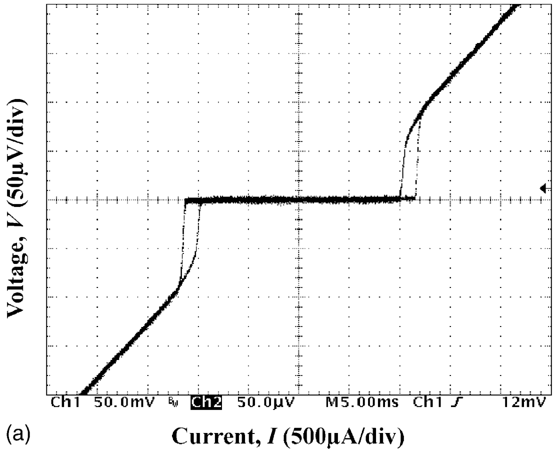

(a)

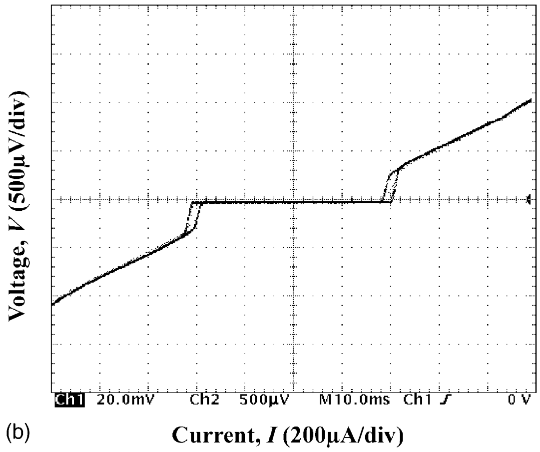

(b)

Fig. 1. I–V characteristics of different designed ramp junctions, (a): Nb/HfTi/Nb trilayer structure, (b): Nb/HfTi–Nb–HfTi/Nb multilayer structure.

Fig. 1a and b show I–V characteristics of single junctions, realized in different structures, Nb/HfTi/Nb (a), and Nb/HfTi–Nb–HfTi/Nb (b). A hysteresis of about 10% was found in most junctions with N-layer thicknesses below 25 nm. $V_c = I_c \times R_N$ and j_c have been calculated from these curves. Fig. 2 shows the temperature dependence of the critical current I_c for both types of junctions. Following the calculations in [2] and [6], at a temperature of $T = 4.2$ K, the coherence length ξ_N was fitted for both cases using the relation

$$I_c = \frac{4}{\pi e R_N} \frac{\Delta^2}{k_B T_c} \frac{d}{\xi_N} \exp\left(-\frac{d}{\xi_N}\right).$$

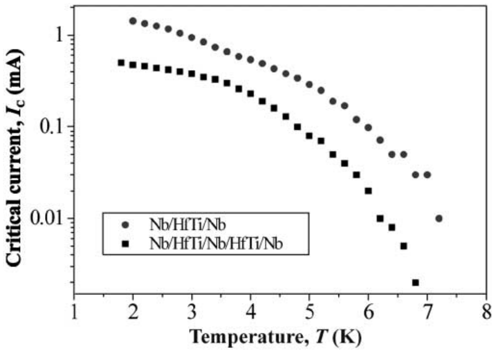

Fig. 2. Dependence of the critical current I_c on the temperature T for Nb/HfTi–Nb–HfTi/Nb ramp junctions.

For HfTi N-layers, a coherence length of $\xi_N = 3.4$ nm has been evaluated and, according to $\rho_N = R_N$ A/d, the resistivity was derived to be $\rho_N = 0.11$ mΩ cm (van der Pauw pattern measurements, $\rho_N = 0.10$ mΩ cm). For Nb/HfTi–Nb–HfTi/Nb junctions, the resistivity was derived to be $\rho_{N'} =$ 1.1 mΩ cm. The measurements show that N′ multilayer structures exhibit a considerable increase in the effective resistivity. We believe that this effect results from the presence of the additional interfaces which is assumed to simultaneously cause a decrease in the critical current density.

Fig. 3 shows the magnetic field dependence of a single Nb/HfTi–Nb–HfTi/Nb contact. The magnetic field was applied perpendicular to the direction of current flow through the junction. The

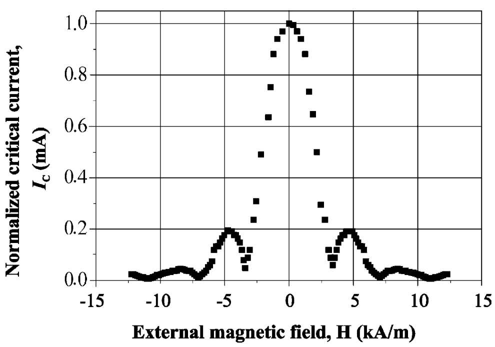

Fig. 3. Dependence of the normalized critical current $I_c/I_{c\,max}$ on a magnetic field H externally applied to a Nb/HfTi–Nb–HfTi/Nb multilayer structure.

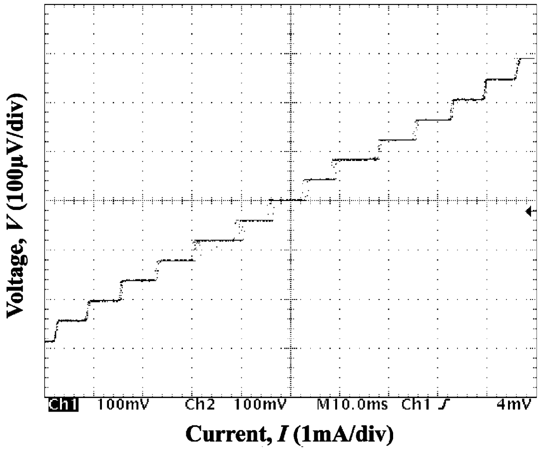

Fig. 4. *I–V* characteristics of Nb/HfTi–Nb–HfTi/Nb ramp junctions under microwave irradiation.

figure indicates a nearly homogeneous current distribution across the junction. Slight deviations from ideal behaviour are due to the particular ramp geometry, as discussed previously [7]. Fig. 4 shows the *I–V* characteristic of the multilayer junction under 20 GHz microwave irradiation. Broad and stable voltage steps are exhibited up to higher orders.

4. Conclusion

We have fabricated and tested different types of Nb based SNS ramp junctions. Between the Nb electrodes we used HfTi as N-barrier material in combination with additional materials, i.e. Al and Nb, and in different layer sequences. The experimental results (measurement temperature $T = 4.2$ K show the influence of inherent layer interfaces on the properties of the junctions. Considerable influence has been found for a Nb/HfTi–Nb–HfTi/Nb multilayer structure of the junction, leading to an increase in the characteristic voltage to $V_c = 460$ µV, while simultaneously reducing the critical current density, $j_c = 210$ kA/cm^2 (compared to $V_c = 107$ µV and $j_c = 550$ kA/cm^2 for a Nb/HfTi/Nb structure). In an externally applied magnetic field, a nearly homogeneous current distribution across the junction is indicated. Under microwave irradiation at 20 GHz, the multilayer junctions exhibit broad constant voltage steps.

Acknowledgements

The work is supported by the Deutsche Forschungsgemeinschaft (DFG), Germany (NI 253/3-1/3-2), the Bundesministerium für Bildung und Forschung (BMBF), Germany (13N6835, 13N7259, 13N7494) and the European Union (SMT4-CT98-2239).

References

[1] R. Pöpel et al., Supercond. Sci. Technol. 13 (2000) 148.
[2] R. Pöpel et al., Inst. Phys. Conf. Ser. 167 (2000) 277.
[3] D. Hagedorn et al., IEEE Trans. Appl. Supercond. 11 (2001) 1134.
[4] R.F. Broom et al., Appl. Phys. Lett. 37 (1980) 237.
[5] J.H. Sasserath et al., J. Vac. Sci. Technol. A 8 (1990) 3914.
[6] K.K. Likharev, Rev. Mod. Phys. 51 (1979) 116.
[7] J.-K. Heinsohn et al., J. Appl. Phys. 90 (2001) 4623.